On the essentials of drought in a changing climate

Toby R. Ault,[1*]

[1]Department of Earth and Atmospheric Science, Cornell University, Ithaca, NY

[*]To whom correspondence should be addressed; E-mail: toby.ault@cornell.edu.

Droughts of the future are likely to be more frequent, severe, and longer lasting than they have been in recent decades, but drought risks will be lower if greenhouse gas emissions are cut aggressively. This review presents a synopsis of the tools required for understanding the statistics, physics, and dynamics of drought and its causes in a historical context. While these tools have been applied most extensively in the US, Europe, and the Amazon region, they have not been as widely used in other drought-prone regions throughout the rest of the world, presenting opportunities for future research. Water resource managers, early career scientists, and veteran drought researchers will likely see opportunities to improve our understanding of drought.

Out of the blue

Unlike most natural disasters, but like a disease, a drought begins before it presents any symptoms (*1*). To understand this, imagine that it is May of 2013 and that you are a farmer in the Caribbean. It has been a little dry recently, but, otherwise, all seems well ahead of the summer rains. The weather is warm, the skies are clear, and the horizon has a yellowish hue from dust carried across the Atlantic from the far-off Sahel (*2*). Although you do not know it yet, the

worst drought in at least half a century has already begun (*2*). Before it is over, it will persist for three years, push two million people into food insecurity, and affect nearly every island in the Caribbean (*2*).

In the US, drought cost $250 billion in damages and killed nearly 3,000 people between 1980 and 2020, making it the costliest natural disaster and the second most deadly one (*3*). Over the last twelve centuries of human civilization, multi-decadal megadroughts contributed to the demise of some of the most complex societies of the pre-industrial era, including the Khmer and Mayan Empires, the Puebloan cliff-dwellers of the southwestern US, and the Yuan Dynasty of China (*4*). The Old Testament vividly describes drought as punishment from God that left "Judah wailing, her cities languishing, the land cracked, and wild donkeys standing on barren heights, panting like jackals." Adding, "Even the doe in the field deserts her newborn fawn because there is no grass" (Jeremiah 14).

Droughts of the future may eclipse those of past centuries in their duration, severity, and frequency (*5, 6*). Although aggressively cutting greenhouse gas emissions reduces these risks, even low levels of warming could amplify drought hazards across much of the world, including the Caribbean, Central America, Brazil, western Europe, central Africa, Southeast Asia, and Australia (*6, 7*).

Defining drought

While the crisis of drought is easily recognized, there is no universally accepted criterion for what constitutes one (*4, 8–10*). Instead, multiple definitions, indices, and metrics exist to meet the particular needs of different research communities or applications (*10*). What they have in common was adroitly articulated by the late Kelly Redmond: they characterize intervals of time when *the supply of moisture fails to meet its demand* (*9*). While the atmosphere delivers the supply of moisture, the demand for it arises from countless sources—a hot, dry atmosphere

demands water vapor from the surface; plants demand water for transpiration; our infrastructure demands water resources for irrigation, municipal water supply, and hydroelectric power generation, among many other uses.

Droughts are classified according to their impact (*8, 10*), which imposes an approximate timescale for each type of drought. A meteorological drought stems from rainfall shortages over a period of weeks, while an agricultural drought exacts crop losses and may linger for months. A hydrological drought develops on seasonal to interannual time horizons by depleting streamflow or reservoir levels.

Socio-economic droughts, which affect water resources required for human applications (e.g., municipal drinking water), arise from either a shortage of supply or an excess of demand (*10*). While the rest of this review will focus on the physics of meteorological and agricultural drought in a changing climate, the basic ideas are broadly relevant to other types of droughts.

An analytical arsenal for drought research

A simple bucket model (eq. 1) builds on the concept of drought as a phenomena that arises from either a shortage of precipitation supply (P) or an excess of evapotranspiration demand (E) (e.g., (*11*) and references therein):

$$P - E = \frac{dS}{dt} + R_o + G_w, \tag{1}$$

Where the terms on the right are changes in soil moisture storage (dS/dt), runoff (R_o), and groundwater flow (G_w) (*11*).

In principle, if we had observations of *P-E*, soil moisture, and runoff going back at least a century, then we could readily characterize drought variability on intra-seasonal to multi-decadal time horizons. In practice, only precipitation measurements are available from the last

few decades, and those records are subject to large uncertainties that affect our understanding of drought (*12*). Measuring evapotranspiration (E) and changes in soil moisture (dS/dt) accurately and consistently across space and through time has vexed drought scientists for generations (*8, 13*).

Drought Indices

As an alternative to measuring soil moisture directly, drought indices track relative departures from normal conditions (*14, 15*). The full palette of drought indices available for researchers and water resource managers is described in other reviews (*8, 10*), and new indices are routinely added to this collection (*16*). Broadly, they fall into two categories: indices that track the supply of moisture from precipitation alone (*17*), and indices that approximate the balance of moisture arising from the combined effects of precipitation, evapotranspiration, and, sometimes, storage (*14, 15*).

The Standardized Precipitation Index (SPI) (*17*) is designed to track precipitation deficits and surpluses across multiple timescales (e.g., 1, 3, or 12 months), thus making it ideal for differentiating between different types of drought (e.g., meteorological versus agricultural). However, the SPI's exclusion of evapotranspiration limits its usefulness for some applications and research questions (*15*). The Standardized Precipitation minus Evapotranspiration Index (SPEI) (*15*) was developed to address this limitation, while preserving the robust statistical features of SPI.

Both the SPI and the SPEI emerged to fill a need for drought indices that was imperfectly carved out by the Palmer Drought Severity Index (PDSI) several decades earlier (*14*). Like the SPEI, PDSI approximates evapotranspiration demand, but it also accounts for moisture storage by different types of soils (*14*). The "self-calibrating" PDSI (*18*) is most appropriate for large scale studies of drought variability and long-term change (*12, 19–21*). Even so, the magnitude

of future change expected from the PDSI depends strongly on its formulation and the historical data used to calibrate it (*21*).

The SPEI and PDSI depend on simplified estimates of potential evapotranspiration (PET) that must be parameterized, and doing so accurately requires meteorological variables beyond precipitation (*12, 21*). Consider the widely-used, physically-based Penman-Montieth equation, which approximates PET as a function of net surface radiation (R_n), soil heat flux (G), water vapor pressure deficit ($e_s - e_a$), the slope of the temperature-saturation vapor pressure relationship (Δ), the psychrometric constant (γ), and two resistance terms (r_s, for surface resistance, and r_a, for atmospheric resistance) (*22*):

$$\mathrm{ET} = \frac{\Delta(\mathrm{R_n} - \mathrm{G}) + \rho_\mathrm{a} \mathrm{c_p} \dfrac{\mathrm{e_s} - \mathrm{e_a}}{\mathrm{r_a}}}{\Delta + \gamma \left(1 + \dfrac{\mathrm{r_s}}{\mathrm{r_a}}\right)}, \tag{2}$$

with ρ_a the density of air and c_p the heat capacity of dry air.

Use of equation (2) requires temperature, humidity, surface pressure, net radiation, and wind speed data (*22*). Of these, only temperature is widely available across large spatial scales and going back more than a few decades (*12*). Employing the Penman-Montieth equation (eq. 2) to study drought at continental scales therefore usually entails merging gridded observational datasets with reanalysis products (*12*); errors in these observational fields will introduce uncertainties into drought indices computed from them (*12*).

Nevertheless, PDSI and SPEI (as well as others) can be computed from observational and model output alike, which, ostensibly, allows projections of the future to be compared against historical conditions using the same indices for both data products (*5, 12, 20, 21*).

Modeling soil moisture

Given the apparent simplicity of equation (1), one might be tempted to model soil moisture di-

rectly using meteorological variables as boundary conditions, thus circumventing the need for drought indices (*11*). For example, the simplified "bucket" model extends global soil moisture estimates back to 1948 (*11*), but it lacks a number of critical processes that affect evapotranspiration including lateral flow and sub-soil storage of moisture the rock layer (*23, 24*).

More sophisticated land surface models (LSMs) assimilate data from multiple sources to estimate historical variations in land-surface hydrology (*25*). However, as with drought indices, observational uncertainties affect the quality of soil moisture data in LSMs (*26*), and appropriate observational boundary conditions only span 1979 to present (*25*). Consequently, LSM output covers a short and heavily forced period of the recent past, which presents a challenge for detecting and attributing the imprint of climate change in soil moisture (*27*).

An advantage of LSMs, however, is that they simulate the moisture, energy, and biogeochemical fluxes between the atmosphere and the land surface, just as the land surface components of general circulation models (GCMs) do. LSMs therefore also serve as an important bridge between observational data and climate model simulations of the past, present, and future.

Finally, over the last decade, observations of soil moisture, from either in situ measurements (*28*) or remote sensing (*29*), have emerged as invaluable tools for validating LSMs and monitoring drought. Yet these products cover a relatively short time period; they do not provide much information about interannual, let alone decadal, variations during the historical period.

Diagnosing drought dynamics

Atmospheric moisture budgets express the local balance of precipitation minus evapotranspiration (P-E) as a function of specific humidity (q) and horizontal winds ($\vec{\mathbf{V}}$) (*30*):

$$P - E = -\frac{1}{g}\left(\frac{\partial \varphi}{\partial t} + \nabla \cdot \int_0^{p_s} q\vec{\mathbf{V}} dp\right) \tag{3}$$

with total precipitable water, φ, defined as the vertical integral of water vapor:

$$\varphi = \int_0^{p_s} q \, dp \, . \tag{4}$$

Changes to the P-E balance of equation (3) must originate from one of two sources: (a) localized fluxes of precipitation or evaporation (the first term inside the parenthesis on the right); or (b) the convergence or divergence of vertically integrated moisture flux (i.e., the second term inside the parenthesis). This second term can be further decomposed to separate changes originating from the mean flow, transport by transient eddies, divergence of the high level winds, and advection of moisture gradients by the lower atmosphere (*30*).

In addition to atmospheric moisture budgets, idealized numerical modeling experiments serve as invaluable tools for investigating the origins of drought (*31*). These experiments typically force a free-running atmosphere with prescribed sea surface temperature (SST) anomalies that are hypothesized to cause drought (*31*). Running multiple atmospheric simulations—all of which are forced with the same SST field—then averaging these simulations together, disentangles the SST "signal" in droughts from the atmospheric "noise."

Causes of drought

The general circulation of the atmosphere delivers moisture from the world's oceans to its continents. Some of that moisture becomes trapped in glaciers, aquifers, and lakes. The rest flows through soils, plants, and rivers. Drought occurs from aberrations to the flow of moisture through these terrestrial systems.

The largest disruptions to the global hydrological cycle occur during El Niño and La Niña events (Fig. 1) (*31–33*). For example, El Niño displaces tropical rainfall in northeast Brazil, Central America, and the Caribbean, causing drought in those regions (*32*) (Fig. 1). Meanwhile, the areas that normally see strong convection—like Indonesia and northern Australia—also

experience rainfall shortages, crop losses, and wildfires (*34, 35*).

While ENSO's impacts on global climate were recognized decades ago, moisture budgets and idealized SST forcing experiments reveal key details of the dynamical processes responsible for those teleconnections (*31, 33*). Winter storms shift equator-ward during El Niño years (*36*) because deep convection modifies the structure and flow of the storm tracks, and hence the transport of moisture (*36*). This, in turn, can trigger drought in the Pacific Northwest and the southeastern US due to additional downstream effects (*36*).

On shorter timescales, seasonal modes of variability, like the North Atlantic Oscillation (NAO), can modify storm tracks crossing the Atlantic (*37*). During the positive phase of the NAO, winter storms crossing the Atlantic tend to make landfall at higher latitudes (e.g., the UK and Scandinavia), which in turn favors drier conditions across France, Spain, Italy and the Mediterranean region in general (*37, 38*).

Over longer timescales, decadal SST variability appears connected to drought (*31*), though it can be difficult to disentangle such long-term affects from anthropogenic forcing (which may also affect decadal SST variations) (*31*).

Lastly, atmospheric moisture budgets also serve as invaluable tools for evaluating the realism of GCMs and for diagnosing their predictions of future aridity (*39*), though this remains a relatively under explored area for future research.

Back to the Future

If you are a water resource manager and you remember just one thing from this review, I hope it is this: cutting CO2 emissions reduces drought risk (*6, 7*). In many regions—including Central America, the Caribbean, the Amazon, Western Europe, and southern Africa—avoiding even just half a degree of warming makes a difference: regional drying is more severe if global warming reaches 2.0^oC than if it is curtailed at 1.5^oC (*6, 7*).

Climate change alters the balance of moisture throughout the world by disrupting its supply through changes in the general circulation (*39, 40*). Meanwhile, higher temperatures can increase moisture demand from the land surface (*12, 41*) for the same reason that a sauna will dry out a towel faster than a steam room (see equation 2). Accordingly, regions seeing both a decrease in supply and an increase in demand are very sensitive to even low levels of warming (*6*).

Plants, however, may use water more efficiently as CO2 concentrations increase in the atmosphere (*42*), and this "CO2 fertilization effect" might partially offset a portion of future drying predicted for some regions (*42–44*). Nevertheless, there are several examples of models that predict reductions in soil moisture despite increases in overall precipitation and an increase in water use efficiency by plants (*5, 42, 44*). That is, the improvements in efficiency from higher CO2 concentrations reduce the total amount of drying—which is substantial—but they do not reverse it (Fig. 3).

Finally, ENSO will likely continue to disrupt hydroclimate across vast spatial scales (*32*). When it does, the impacts of El Niño on drought could be even more severe than they are today for two reasons: (1) we expect climate change to strengthen ENSO events (*45, 46*); and (2) a hotter atmosphere demands more moisture from the land surface when droughts occur (*41, 47*). Even now, higher temperatures may already be worsening aridity beyond anything seen in the last few centuries (*27*).

The future of drought research

Legions of studies have used the analytical arsenal described earlier to confront fundamental questions about the physics, dynamics, and risks of drought in a changing climate. For example, they have asked:

1. How do future droughts and long-term changes in aridity compare to modern-day con-

ditions? (*19–21, 41*) Which indices and models should be used to characterize future droughts? (*21, 42, 43*) Is there already a *detectable* imprint of anthropogenic climate change on global drought? (*19, 20, 27*)

2. How will regional changes in temperature affect moisture demand from the atmosphere through evapotranspiration? (*42, 43*) What role does vegetation play in coupling the land-surface to the atmosphere? (*42–44*)

3. How will the supply of moisture to land evolve in response to large-scale changes in the general circulation? (*39*) How will ENSO and other seasonal variations influence drought in the future? (*46, 48*)

In addressing these questions, researchers have begun assembling the puzzle of drought risks in a changing climate. Many regions may face events that are more severe, frequent, and long-lasting than those of the recent past (*13, 21, 26*), or even the last millennium (*4, 5, 27*). However, not all of the pieces fit together.

Wet hot American summer drought

Perhaps the most contentious debate among drought researchers stems from differences between drought indices (as described in Section) computed from GCMS and soil moisture simulated by those same models. Drought indices depict unprecedented drying throughout much of the US (*5, 20, 21*). But, those indices do not account for biological processes (like CO2 uptake) that may alter the surface moisture balance in the future (*42, 43*). They are also sensitive to the length and quality of historical data used to calibrate them (*12, 21*), and they may distort the magnitude of future changes if they are not calibrated appropriately (*12, 19–21*). Lastly, their reliance on the Penman-Montieth equation might overestimate future PET rates (*43*).

Soil moisture projections from LSMs help characterize some limitations of drought indices,

although they too have their own pitfalls. For example, soil moisture data is not widely available in most regions, making it difficult to directly compare LSM output against the historical record (*26*). LSMs typically overestimate evapotranspiration rates (*49*), which in turn makes them too strongly coupled to the atmosphere, and artificially enhances precipitation in some regions (*49*). Although they can simulate CO2 "fertilization" in plants, their modules for representing ecological interactions between plants, soil moisture, and runoff all introduce new uncertainties that propagate into their projections of the future (*26, 44*).

While GCM-based drought indices and soil moisture variables do not paint an entirely consistent picture of future drying, their differences may be superficial (*44*) (Fig 3). In the case of the Community Earth System Model (CESM) "large ensemble" (*50*), the apparent paradox of increased drought risk in a wetter climate is easy to reconcile: most of the increase in precipitation occurs during the winter, whereas most of the drying occurs during the summer (Fig. 3). From the perspective of soil moisture balance (Fig. 3, bottom panel), the increase in demand for evaporation (from higher temperatures) exceeds the increase in supply from precipitation. Future research could elaborate on these details in other models and other parts of the world.

Expanding outward

Quantifying how uncertainties in the large-scale circulation of GCMs are manifest in regional predictions of drought presents a harder problem for researchers (*51*). For example, GCMs simulations of the 21st century depict a scenario where the subtropics become drier, while wet equatorial regions become rainier (*40*) (Fig. 2). In a general sense, this sub-tropical drying is a robust thermodynamic response to higher temperatures: a warmer atmosphere can "hold" more water vapor, yet the rate at which water vapor increases in the atmosphere outpaces the rate of precipitation increase (*39, 40*). Accordingly, less moisture evaporates from the ocean to meet the demand for precipitation, which slows tropical circulation (*40*).

Most of the slowdown in tropical circulation occurs in the meridional Hadley cells, causing them to widen (*40*), which dries the sub-tropics. GCMs predict a similar outcome over the tropical Pacific Ocean because the east-west Walker circulation should also slow down in conjunction with the Hadley cells (*52*).

But this isn't happening (*53*). Or, if it is happening, recent trends in the historical record are being dominated by other processes. One possible cause for this discrepancy is that the Walker circulation is responding differently in reality than in models to greenhouse gas forcings (*48*). That is, the recent observed changes are a forced dynamical adjustment in the coupled ocean-atmosphere system that the GCMs do not capture (*48*).

Alternatively, substantial internal *decadal* variability in the equatorial Pacific Ocean may be overshadowing the forced response of the Walker Circulation (*54*). On this point, models do not agree with each other–let alone the observations–on the relative importance of decadal variability in the tropical Pacific (Fig. 4).

For the time being, the issue must be regarded as unresolved. Yet, its resolution is vital to our portrait of 21st century drought risk because the structure of the Walker circulation affects rainfall throughout the world (*39*).

The issues described above will manifest in the mean moisture balance of the tropics and subtropics, but droughts of the future will be caused by both the long-term changes in the general circulation and short-term deviations during El Niño and La Niña events (in addition to other modes of climate variability). Importantly, GCMs do not agree with one another, let alone the historical record, on the amplitude of ENSO fluctuations and the relative importance of decadal variability (Fig. 4) (*55, 56*). Since the tropical Pacific exerts a major influence on global precipitation patterns (*32*) (Fig. 1), frequency biases in this region likely affect the statistics of precipitation in regions with strong ENSO teleconnections. Quantifying the relationship between ENSO frequency biases in GCMS (as well as potential changes in ENSO frequency) and

drought presents an important area for future research.

New additions to the analytical arsenal

During the last 30 years, intellectual and technological breakthroughs accelerated the pace of drought research. In the 1990s, personal computers enabled scientists to develop, analyze, and deploy our current generation of drought indices. In the early 2000s, investments in high performance computing and land surface models helped lay the foundation for the sophisticated LSMs used today. In the 2010s, satellites began making unprecedented global measurements of surface soil moisture (*29*). While all these technologies brought powerful tools into our analytical arsenal, they are not very egalitarian. Most farmers living in the Majority World must confront the hazards of drought in a changing climate with little, if any, access to the technological advancements of recent decades.

Encouragingly, the late 2010s also introduced very low-cost soil moisture sensors, which are already being deployed through public partnerships with local communities (*57*). These sensors transmit information about the state of the land surface continuously and nearly instantaneously, and researchers can use this data to validate satellite retrievals, initialize near-term predictions, or study the flow of moisture through the land surface with an unprecedented density of *in situ* measurements. At the same time, local communities are able to use data from those devices to gain insight into current conditions. During the 2020s, this emerging "Internet-of-things" technology could become the new frontier of drought monitoring and modeling.

Imagine, again, that you are a farmer in the Caribbean during a drought, but this time the year of 2035. It is exceptionally hot (*7*), aquifers are depleted (*58*), and there are frequent blackouts because reservoir levels are so low at the hydroelectric power plant (*59*). What would you ask us—the people alive today—to do now to ensure that you are resilient in the face of drought in a changing climate?

References

1. I. R. Tannehill, *Drought: Its causes and consequences*. Princeton, NJ: Princeton University Press, 1947.

2. D. A. Herrera, T. R. Ault, J. T. Fasullo, S. J. Coats, C. M. Carrillo, B. I. Cook, and A. P. Williams, "Exacerbation of the 2013-2016 Pan-Caribbean Drought by Anthropogenic Warming," *Geophysical Research Letters*, vol. 45, oct 2018.

3. A. B. Smith and J. L. Matthews, "Quantifying uncertainty and variable sensitivity within the US billion-dollar weather and climate disaster cost estimates," *Natural Hazards*, vol. 77, pp. 1829–1851, jul 2015.

4. B. I. Cook, E. R. Cook, J. E. Smerdon, R. Seager, A. P. Williams, S. Coats, D. W. Stahle, and J. V. Díaz, "North American megadroughts in the Common Era: reconstructions and simulations," *Wiley Interdisciplinary Reviews: Climate Change*, vol. 7, pp. 411–432, mar 2016.

5. B. I. Cook, T. R. Ault, and J. E. Smerdon, "Unprecedented 21st century drought risk in the American Southwest and Central Plains," *Science Advances*, vol. 1, no. February, pp. 1–7, 2015.

6. F. Lehner, S. Coats, T. F. Stocker, A. G. Pendergrass, B. M. Sanderson, C. C. Raible, and J. E. Smerdon, "Projected drought risk in 1.5C and 2C warmer climates," *Geophysical Research Letters*, vol. 44, pp. 7419–7428, jul 2017.

7. M. A. Taylor, L. A. Clarke, A. Centella, A. Bezanilla, T. S. Stephenson, J. J. Jones, J. D. Campbell, A. Vichot, and J. Charlery, "Future Caribbean Climates in a World of Rising

Temperatures: The 1.5 vs 2.0 Dilemma," *Journal of Climate*, vol. 31, pp. 2907–2926, apr 2018.

8. D. A. Wilhite, *Chapter 1 Drought as a Natural Hazard: Concepts and Definitions*. Lincoln, NE: Drought Mitigation Center Faculty Publications, 2000.

9. K. T. Redmond, "The depiction of drought - A commentary," *Bulletin of the American Meteorological Society*, vol. 83, no. 8, pp. 1143–1147, 2002.

10. A. K. Mishra and V. P. Singh, "A review of drought concepts," *Journal of Hydrology*, vol. 391, pp. 204–216, sep 2010.

11. Y. Fan and H. van den Dool, "Climate Prediction Center global monthly soil moisture data set at 0.5 degrees resolution for 1948 to present," *Journal of Geophysical Research-atmospheres*, vol. 109, may 2004.

12. A. Dai and T. Zhao, "Uncertainties in historical changes and future projections of drought. Part I: estimates of historical drought changes," *Climatic Change*, vol. 144, pp. 519–533, oct 2017.

13. A. Dai, T. Zhao, and J. Chen, "Climate Change and Drought: a Precipitation and Evaporation Perspective," *Current Climate Change Reports*, vol. 4, pp. 301–312, sep 2018.

14. W. M. Alley, "The Palmer Drought Severity Index - Limitations and Assumptions," *Journal of Climate and Applied Meteorology*, vol. 23, no. 7, pp. 1100–1109, 1984.

15. S. M. Vicente-Serrano, S. Beguería, and J. I. López-Moreno, "A multiscalar drought index sensitive to global warming: The standardized precipitation evapotranspiration index," *J. Clim.*, vol. 23, no. 7, pp. 1696–1718, 2010.

16. Z. Hao and A. AghaKouchak, "Multivariate Standardized Drought Index: A parametric multi-index model," *Advances in Water Resources*, vol. 57, pp. 12–18, jul 2013.

17. N. B. Guttman, "Accepting the standardized precipitation index: A calculation algorithm," *Journal of the American Water Resources Association*, vol. 35, no. 2, pp. 311–322, 1999.

18. N. Wells, S. Goddard, and M. J. Hayes, "A self-calibrating Palmer Drought Severity Index," *Journal of Climate*, vol. 17, no. 12, pp. 2335–2351, 2004.

19. J. Sheffield, E. F. Wood, and M. L. Roderick, "Little change in global drought over the past 60 years," *Nature*, vol. 491, pp. 435+, nov 2012.

20. A. Dai, "Increasing drought under global warming in observations and models," *Nature Climate Change*, vol. 3, pp. 52–58, jan 2013.

21. K. E. Trenberth, A. Dai, G. van der Schrier, P. D. Jones, J. Barichivich, K. R. Briffa, and J. Sheffield, "Global warming and changes in drought," *Nature Climate Change*, vol. 4, pp. 17–22, jan 2014.

22. R. G. Allen, L. S. Pereira, D. Raes, and M. Smith, "Crop evapotranspiration-Guidelines for computing crop water requirements-FAO Irrigation and drainage paper 56," tech. rep., 1998.

23. R. M. Maxwell and L. E. Condon, "Connections between groundwater flow and transpiration partitioning," *Science*, vol. 353, pp. 377–380, jul 2016.

24. D. M. Rempe and W. E. Dietrich, "Direct observations of rock moisture, a hidden component of the hydrologic cycle," *Proceedings of the National Academy of Sciences of the United States of America*, vol. 115, pp. 2664–2669, mar 2018.

25. M. Rodell, P. R. Houser, U. Jambor, J. Gottschalck, K. Mitchell, C. J. Meng, K. Arsenault, B. Cosgrove, J. Radakovich, M. Bosilovich, J. K. Entin, J. P. Walker, D. Lohmann, and D. Toll, "The Global Land Data Assimilation System," *Bulletin of the American Meteorological Society*, vol. 85, pp. 381–394, mar 2004.

26. A. Berg and J. Sheffield, "Climate Change and Drought: the Soil Moisture Perspective," *Current Climate Change Reports*, vol. 4, pp. 180–191, jun 2018.

27. K. Marvel, B. I. Cook, C. J. Bonfils, P. J. Durack, J. E. Smerdon, and A. P. Williams, "Twentieth-century hydroclimate changes consistent with human influence," *Nature*, vol. 569, pp. 59–65, may 2019.

28. W. A. Dorigo, W. Wagner, R. Hohensinn, S. Hahn, C. Paulik, A. Xaver, A. Gruber, M. Drusch, S. Mecklenburg, P. Van Oevelen, A. Robock, and T. Jackson, "Hydrology and Earth System Sciences The International Soil Moisture Network: a data hosting facility for global in situ soil moisture measurements," *Hydrol. Earth Syst. Sci*, vol. 15, pp. 1675–1698, 2011.

29. D. Entekhabi, E. G. Njoku, P. E. O'Neill, K. H. Kellogg, W. T. Crow, W. N. Edelstein, J. K. Entin, S. D. Goodman, T. J. Jackson, J. Johnson, J. Kimball, J. R. Piepmeier, R. D. Koster, N. Martin, K. C. McDonald, M. Moghaddam, S. Moran, R. Reichle, J. C. Shi, M. W. Spencer, S. W. Thurman, L. Tsang, and J. Van Zyl, "The Soil Moisture Active Passive (SMAP) Mission," *Proceedings of the IEEE*, vol. 98, pp. 704–716, may 2010.

30. K. E. Trenberth and C. J. Guillemot, "Evaluation of the global atmospheric moisture budget as seen from analyses," *Journal of Climate*, vol. 8, pp. 2255–2272, sep 1995.

31. S. D. Schubert, R. E. Stewart, H. Wang, M. Barlow, E. H. Berbery, W. Cai, M. P. Hoerling, K. K. Kanikicharla, R. D. Koster, B. Lyon, A. Mariotti, C. R. Mechoso, O. V. Müller,

B. Rodriguez-Fonseca, R. Seager, S. I. Senevirante, L. Zhang, and T. Zhou, "Global meteorological drought: A synthesis of current understanding with a focus on sst drivers of precipitation deficits," *Journal of Climate*, vol. 29, pp. 3989–4019, jun 2016.

32. A. Dai and T. M. L. Wigley, "Global patterns of ENSO-induced precipitation," *Geophysical Research Letters*, vol. 27, pp. 1283–1286, may 2000.

33. K. E. Trenberth, J. Fasullo, and L. Smith, "Trends and variability in column-integrated atmospheric water vapor," *Climate Dynamics*, vol. 24, pp. 741–758, jun 2005.

34. J.-H. Qian, A. W. Robertson, and V. Moron, "Interactions among ENSO, the Monsoon, and Diurnal Cycle in Rainfall Variability over Java, Indonesia," *Journal of the Atmospheric Sciences*, vol. 67, pp. 3509–3524, nov 2010.

35. N. Zeng, A. Mariotti, and P. Wetzel, "Terrestrial mechanisms of interannual CO 2 variability," *Global Biogeochemical Cycles*, vol. 19, mar 2005.

36. R. Seager, N. Naik, M. Ting, M. A. Cane, N. Harnik, and Y. Kushnir, "Adjustment of the atmospheric circulation to tropical Pacific SST anomalies: Variability of transient eddy propagation in the Pacific-North America sector," *Quarterly Journal of the Royal Meteorological Society*, vol. 136, pp. 277–296, jan 2010.

37. J. W. Hurrell, "Decadal trends in the North Atlantic oscillation: Regional temperatures and precipitation," *Science*, vol. 269, no. 5224, pp. 676–679, 1995.

38. J. I. López-Moreno and S. M. Vicente-Serrano, "Positive and Negative Phases of the Wintertime North Atlantic Oscillation and Drought Occurrence over Europe: A Multitemporal-Scale Approach," *Journal of Climate*, vol. 21, pp. 1220–1243, mar 2008.

39. R. Seager, N. Naik, and G. A. Vecchi, "Thermodynamic and Dynamic Mechanisms for Large-Scale Changes in the Hydrological Cycle in Response to Global Warming," *Journal of Climate*, vol. 23, pp. 4651–4668, sep 2010.

40. I. M. Held and B. J. Soden, "Robust responses of the hydrological cycle to global warming," *Journal of Climate*, vol. 19, pp. 5686–5699, nov 2006.

41. B. I. Cook, J. E. Smerdon, R. Seager, and S. Coats, "Global warming and 21 st century drying," *Climate Dynamics*, vol. 43, no. 9-10, pp. 2607–2627, 2014.

42. A. L. S. Swann, F. M. Hoffman, C. D. Koven, and J. T. Randerson, "Plant responses to increasing CO2 reduce estimates of climate impacts on drought severity," *Proceedings of the National Academy of Sciences*, 2016.

43. P. C. Milly and K. A. Dunne, "Potential evapotranspiration and continental drying," *Nature Climate Change*, vol. 6, pp. 946–949, sep 2016.

44. J. S. Mankin, J. E. Smerdon, B. I. Cook, A. P. Williams, and R. Seager, "The Curious Case of Projected Twenty-First-Century Drying but Greening in the American West," *Journal of Climate*, vol. 30, pp. 8689–8710, nov 2017.

45. W. Cai, G. Wang, A. Santoso, M. J. McPhaden, L. Wu, F.-F. Jin, A. Timmermann, M. Collins, G. Vecchi, M. Lengaigne, M. H. England, D. Dommenget, K. Takahashi, and E. Guilyardi, "Increased frequency of extreme La Nina events under greenhouse warming," *Nature Climate Change*, vol. 5, pp. 132–137, feb 2015.

46. J. T. Fasullo, B. L. Otto-Bliesner, and S. Stevenson, "ENSO's Changing Influence on Temperature, Precipitation, and Wildfire in a Warming Climate," *Geophysical Research Letters*, vol. 45, pp. 9216–9225, sep 2018.

47. J. E. Herrera-Estrada and J. Sheffield, "Uncertainties in future projections of summer droughts and heat waves over the contiguous United States," *Journal of Climate*, vol. 30, pp. 6225–6246, aug 2017.

48. R. Seager, M. Cane, N. Henderson, D. E. Lee, R. Abernathey, and H. Zhang, "Strengthening tropical Pacific zonal sea surface temperature gradient consistent with rising greenhouse gases," jul 2019.

49. B. Mueller and S. I. Seneviratne, "Systematic land climate and evapotranspiration biases in CMIP5 simulations," *Geophysical Research Letters*, vol. 41, pp. 128–134, jan 2014.

50. J. E. Kay, C. Deser, A. Phillips, A. Mai, C. Hannay, G. Strand, J. M. Arblaster, S. C. Bates, G. Danabasoglu, J. Edwards, M. Holland, P. Kushner, J.-F. Lamarque, D. Lawrence, K. Lindsay, A. Middleton, E. Munoz, R. Neale, K. Oleson, L. Polvani, and M. Vertenstein, "The Community Earth System Model (CESM) Large Ensemble Project: A Community Resource for Studying Climate Change in the Presence of Internal Climate Variability," *Bulletin of the American Meteorological Society*, p. 141119125353005, nov 2014.

51. C. Wang, L. Zhang, S. K. Lee, L. Wu, and C. R. Mechoso, "A global perspective on CMIP5 climate model biases," *Nature Climate Change*, vol. 4, no. 3, pp. 201–205, 2014.

52. G. a. Vecchi, B. J. Soden, A. T. Wittenberg, I. M. Held, A. Leetmaa, and M. J. Harrison, "Weakening of tropical Pacific atmospheric circulation due to anthropogenic forcing.," *Nature*, vol. 441, pp. 73–6, may 2006.

53. M. L. L'Heureux, S. Lee, and B. Lyon, "Recent multidecadal strengthening of the Walker circulation across the tropical Pacific," *Nature Climate Change*, vol. 3, pp. 571–576, mar 2013.

54. E. S. Chung, A. Timmermann, B. J. Soden, K. J. Ha, L. Shi, and V. O. John, "Reconciling opposing Walker circulation trends in observations and model projections," *Nature Climate Change*, vol. 9, pp. 405–412, may 2019.

55. T. R. Ault, J. E. Cole, and S. St. George, "The amplitude of decadal to multidecadal variability in precipitation simulated by state-of-the-art climate models," *Geophys. Res. Lett.*, vol. 39, p. L21705, nov 2012.

56. L. Parsons, G. Loope, J. Overpeck, T. Ault, R. Stouffer, and J. Cole, "Temperature and precipitation variance in CMIP5 simulations and paleoclimate records of the last millennium," *Journal of Climate*, vol. 30, no. 22, 2017.

57. M. Karamouz, A. Ghomlaghi, R. S. Alipour, M. Nazari, and M. Fereshtehpour, "Soil Moisture Data: From Using Citizen Science to Satellite Technology," in *World environmental and water resources congress 2019: emerging and innovative technologies and international perspectives* (W. Scott, GF and Hamilton, ed.), (UNITED ENGINEERING CENTER, 345 E 47TH ST, NEW YORK, NY 10017-2398 USA), pp. 85–95, Environm & Water Resources Inst; Amer Soc Civil Engineers, Environm & Water Resources Inst; Amer Soc Civil Engineers, AMER SOC CIVIL ENGINEERS, 2019.

58. S. Holding, D. M. Allen, S. Foster, A. Hsieh, I. Larocque, J. Klassen, and S. C. Van Pelt, "Groundwater vulnerability on small islands," *Nature Clim. Change*, vol. advance on, sep 2016.

59. FAO, "Drought characteristics and management in the Caribbean," tech. rep., Food and Agriculture Organization of the United Nations, Rome, 2016.

Figures

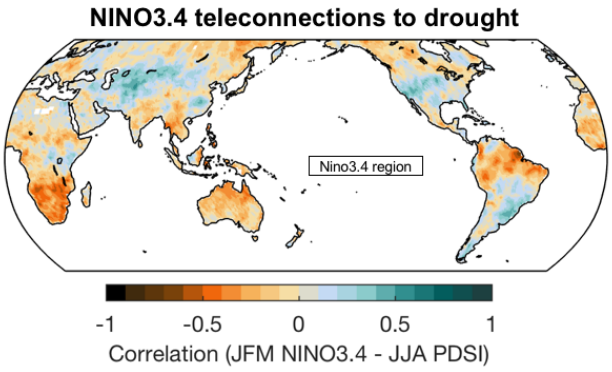

Figure 1: Correlation coefficients between NINO3.4 SST (ERSSTv3b) and self-calibrating PDSI (*19*). All correlations are computed between boreal winter (JFM) SSTs with PDSI during the following boreal summer (JJA).

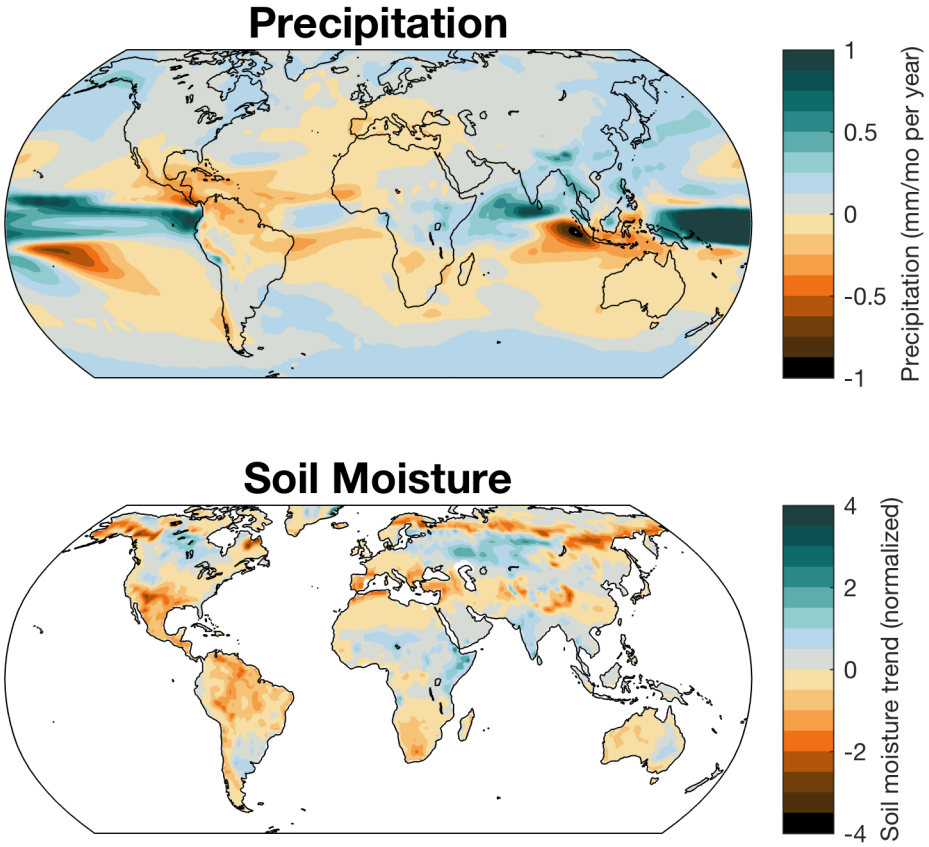

Figure 2: Ensemble-averaged 21st century CMIP5 trends computed from annual precipitation (top) and column-integrated soil moisture (bottom).

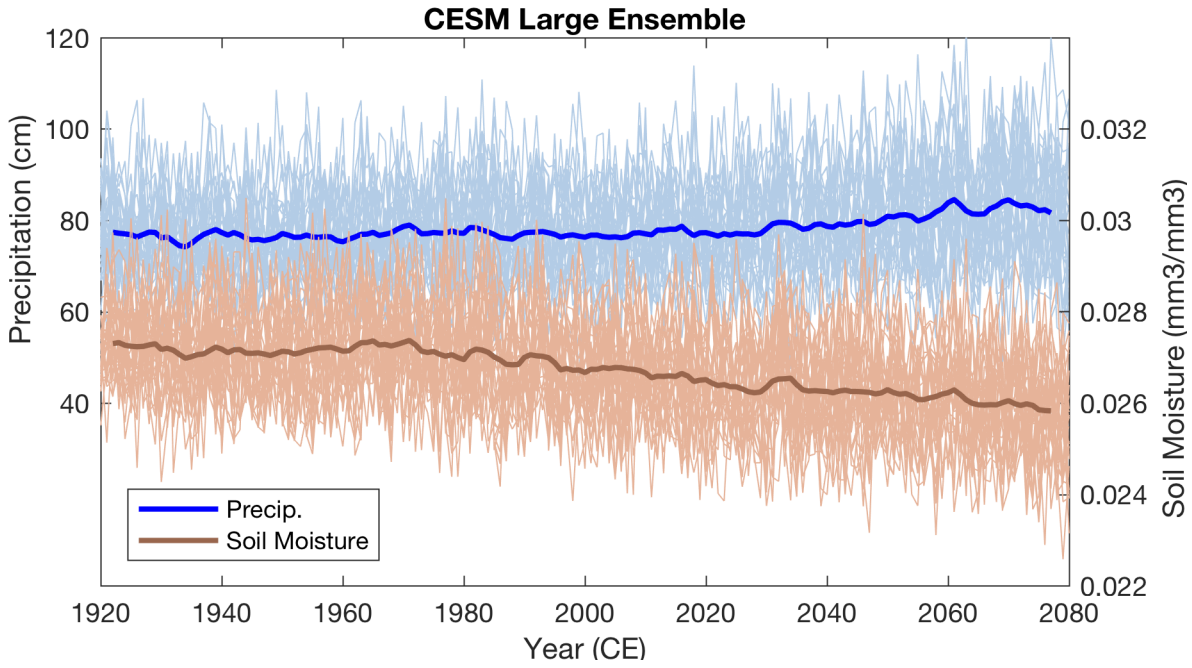

Figure 3: Annual precipitation totals (blue) and JJA volumetric soil moisture averages (brown) from the CESM large ensemble (*50*).

Figure 4: Summary of tropical pacific variability in observations and models. The circle in the topmost left is derived from observational data, with the radius being proportional to the standard deviation ($\pm 1.5^o$C) of NINO3.4, and the lighter color representing the fraction of the total variance that occurs on decadal timescales in the NINO3.4 region (about 8.5%). The remaining charts summarize this same information for individual members of the Climate Model Inter-comparison Project V (CMIP5). Again, the radii of each circle is proportional to the standard deviation of a given model, and the lighter color represents the fraction of total variance occurring on decadal time horizons. For reference, the outline of the observational NINO3.4 chart is included on each model diagram. Variability in circle size emphasizes the now well-known differences in El Niño/Southern Oscillation amplitudes across the CMIP5 archive. Differences in the fraction of variance occurring on decadal timescales—in conjunction with differences in ENSO amplitudes—have received less attention. The models are identified by a single letter as follows: (a) ACCESS1.3; (b) BNU-ESM; (c) CCSM4; (d) CESM1-BGC; (e) CESM1(CAM5-FV2); (f) CESM1(CAM5); (g) CESM1(FASTCHEM; (h) CESM1(WACCM); (i) CMCC-CESM; (j) CMCC-CMS; (k) CMCC-CM; (l) CNRM-CM5-2; (m) CNRM-CM5; (n) CSIRO-Mk3.6.0; (o) CanCM4; (p) CanESM2; (q) EC-EARTH; (r) FGOALS-g2; (s) FIO-ESM; (t) GFDL-CM2.1; (u) GFDL-CM3; (v) GFDL-ESM2G; (w) GFDL-ESM2M; (x) GISS-E2-H-CC; (y) GISS-E2-H; (z) GISS-E2-R-CC; (A) GISS-E2-R; (B) HadCM3; (C) HadGEM2-AO; (D) HadGEM2-CC; (E) HadGEM2-ES; (F) IPSL-CM5A-LR; (G) IPSL-CM5A-MR; (H) IPSL-CM5B-LR; and (I) MIROC-ESM-CHEM. When multiple realizations were available, only the first simulation was used.

Acknowledgments

I thank Dimitris H. Herrera, Colin P. Evans, Marc J. Alessi, Charles R. Ault, Phyllis C. Ault, and Rick Moore for their helpful comments and feedback on the content covered by this review. **Funding:** This effort was partially supported by a National Science Foundation (NSF) grant (1602564) and an NSF CAREER award (1751535). **Author contributions:** I established the scope of this review, wrote all components of the paper, and generated all figures with code that I also wrote. **Competing interests:** None. **Data and materials availability:** Data used for the figures in this review originate from public archives as follows: **Figure 1:** Global gridded PDSI data from (*19*) were obtained from Princeton University's Terrestrial Hydrology Research Group's public data repository ($https://hydrology.princeton.edu/data.pdsi.php$), and NINO3.4 SST data was download from the ESRL PSD Climate Indices page ($https://www.esrl.noaa.gov/psd/data/climateindices/list/$). **Figure 2:** All CMIP5 soil moisture data were downloaded from the Earth System Grid Federation node operated by the Lawrence Livermore National Lab ($https://esgf-node.llnl.gov/projects/cmip5/$). **Figure 3:** Soil moisture data from the CESM large ensemble is available from NCAR's ESG node ($https://www.earthsystemgrid.org/dataset/ucar.cgd.ccsm4.CESM_CAM5_BGC_LE.lnd.proc.monthly_ave.html$). **Figure 4:** NINO3.4 time series used for this figure were also derived from the CMIP5 archive, but were downloaded from NCAR's public repository of Climate Variability Diagnostic Package output ($http://webext.cgd.ucar.edu/Multi-Case/CVDP_ex/CMIP5-Historical/$).